

## Comparison between the frequencies of FML and composite cylindrical shells using beam modal function model

Ahmad Reza Ghasemi<sup>a,\*</sup>, Masood Mohandes<sup>a</sup>

<sup>a</sup> Department of Solid Mechanics, Faculty of Mechanical Engineering, University of Kashan, Kashan, Iran

### ARTICLE INFO

#### Article history:

Received: 24 November 2017

Accepted: 08 January 2018

#### Keywords:

Free Vibration

FML

Circular Cylindrical Shell

Beam Modal Function

Different Lay-ups

### ABSTRACT

A comparison between the vibration of fiber-metal laminate (FML) and composite cylindrical shells has been studied in this manuscript. Love's first approximation shell theory has been applied to obtain Strain-displacement relations. In addition, beam modal function model has been used to analyze the cylindrical shell with different boundary conditions. In this manuscript, the frequencies of FML and composite cylindrical shells have been compared to each other for different materials, lay-ups, boundary conditions, axial and circumferential wave numbers. The most commercially available FMLs are CARALL (carbon reinforced aluminium laminate), and GLARE (glass reinforced aluminium laminate), which are studied in this research. The results showed although the frequencies of carbon/epoxy are greater than glass/epoxy for all of the  $n$ , this process is not constant for FML. Also, with increasing the  $n$ , the frequencies of FML cylindrical shells are converged more faster than the composite one. Moreover, the frequencies of both boundary conditions are converged with increasing  $n$  for both FML and composite cylindrical shells.

### 1. Introduction

Due to some advantages of composite materials such as high value of stiffness and strength to weight ratios, composite structures are used in advanced industries such as aerospace and mechanical especially automobile engineering structures. Some of the other advantages of composite materials are controlling the elastic and structural coupling by fiber orientations and different lay-ups. Composite materials can be classified according to type, geometry and orientation of the reinforcement fibers. Considering free vibration and buckling of composite structures such as beams [1-4] plates [5-6] and cylindrical shells [7-9] has attracted much attention over the past decades. In 2014, free vibration analysis of composite laminated cylindrical shells using the Haar wavelet method subjected to different boundary conditions was studied by Xie et al. [10]. In 2016, Song et al. [11] investigated free and forced vibrations of composite closed cylindrical shells reinforced by CNTs subjected to thermal influences based on Reddy's higher order shear deformation theory. In 2016, Ansari and Torabi [12] employed generalized differential quadrature (GDQ) method in axial direction and periodic differential operators in circumferential direction to study buckling and vibration of axially-compressed functionally graded carbon nanotube-reinforced composite (FG-CNTRC) conical shells according to first order shear deformation theory. The results showed that volume fraction and CNTs distribution had remarkable influence on the buckling and vibration of FG-

CNTRC conical shells subjected to axial loadings. In 2014, Xiang et al. [13] used Haar wavelet discretization method to study free vibration of composite laminated conical, cylindrical shells and annular plates subjected to different boundary conditions based on the first order shear deformation theory. In 2015, Tornabene et al. [14] proposed generalized differential quadrature method for studying free vibration of laminated cylinders of oval and elliptic cross-sections.

A new advanced hybrid composite material is FML which is composed by alternately thin metal with adhesive fiber prepreg. In the past decades, the FMLs have been used in mechanical and aerospace industries due to good characteristics of the metal such as ductility, impact and damage tolerances as well as benefits of the fiber composite materials such as high strength and stiffness to weight ratios, excellent fatigue resistance and acceptable corrosion. Studies on the FMLs are not widespread. Several researches, which have been conducted on the vibrational behavior of different structures, are presented in this literature review. In 2016, Bidgoli and Heidari-Rarani [15] analyzed buckling of an FML cylindrical shell subjected to axial compression by Navier and finite element methods. The effects of volume fraction of metal, fiber orientation, and geometry parameters on the buckling of FML cylindrical shell were discussed. They found that with growing the volume fraction of metal, the buckling load increased. In addition, they indicated that with raising the length and radius of shell, first the buckling

\* Corresponding author. e-mail: [ghasemi@kashanu.ac.ir](mailto:ghasemi@kashanu.ac.ir)

load was grown and then it was declined. In 2017, Mohandes et al. [16] have studied free vibration of FML cylindrical shells subjected to different boundary conditions using beam modal function model. The variation of frequencies of FML circular cylindrical shell for different material properties of composite fiber, volume fraction of composite, fiber orientation, axial and circumferential wave numbers and boundary conditions have been studied. In 2017, Ghasemi and Mohandes [17] have investigated free vibration of rotating FML cylindrical shells. The effects of rotational speeds, axial and circumferential wave numbers, length to radius ratio and metal thickness on the vibration of rotating FML circular cylindrical shells. As predicted, the backward wave frequencies were greater than the forward ones due to the coriolis effect.

In this research, the vibration of FML and composite cylindrical shells has been compared to each other for different boundary conditions by beam modal function method. The composite and FML cylindrical shells are used in pharmaceutical industry as a rotating cylindrical shell that the vibration behavior of them is so important. The results show that the frequencies of carbon/epoxy are greater than glass/epoxy for all of the n in the composite cylindrical shell, but this process is not constant for FML. Also, as grown the n, the frequencies of FML cylindrical shells are converged more speed than the composite one.

**2. Fundamental equations**

The equations of motion for thin circular cylindrical shells are specified as [16]:

$$N_{x,x} + \frac{1}{R} N_{x\theta,\theta} - \rho h \ddot{u} = 0 \tag{1a}$$

$$N_{x\theta,x} + \frac{1}{R} N_{\theta,\theta} + \frac{1}{R} M_{x\theta,x} + \frac{1}{R^2} M_{\theta,\theta} - \rho h \ddot{v} = 0 \tag{1b}$$

$$M_{x,xx} + \frac{2}{R} M_{x\theta,x\theta} + \frac{1}{R^2} M_{\theta,\theta\theta} - \frac{1}{R} N_{\theta} - \rho h \ddot{w} = 0 \tag{1c}$$

where *h* is thickness of the cylindrical shell. Forces *N<sub>ij</sub>* and moments *M<sub>ij</sub>* are stress resultants which are given on the basis of middle surface strains and changes in the curvature and torsion of the middle surface by:

$$\begin{bmatrix} N_x \\ N_\theta \\ N_{x\theta} \\ M_x \\ M_\theta \\ M_{x\theta} \end{bmatrix} = \begin{bmatrix} A_{11} & A_{12} & A_{16} & B_{11} & B_{12} & B_{16} \\ A_{12} & A_{22} & A_{26} & B_{12} & B_{22} & B_{26} \\ A_{16} & A_{26} & A_{66} & B_{16} & B_{26} & B_{66} \\ B_{11} & B_{12} & B_{16} & D_{11} & D_{12} & D_{16} \\ B_{12} & B_{22} & B_{26} & D_{12} & D_{22} & D_{26} \\ B_{16} & B_{26} & B_{66} & D_{16} & D_{26} & D_{66} \end{bmatrix} \begin{bmatrix} \varepsilon_{x,0} \\ \varepsilon_{\theta,0} \\ \varepsilon_{x\theta,0} \\ k_x \\ k_\theta \\ k_{x\theta} \end{bmatrix} \tag{2}$$

where  $\varepsilon_{x,0}$ ,  $\varepsilon_{\theta,0}$  and  $\gamma_{x\theta,0}$  are the middle surface strains and  $k_x$ ,  $k_\theta$  and  $k_{x\theta}$  are the changes in the curvature and torsion of the middle surface. *A<sub>ij</sub>*, *B<sub>ij</sub>* and *D<sub>ij</sub>* are extensional, coupling and bending stiffnesses.

The middle surface strains based on the Love's first approximation shell theory [16] can be expressed as follows:

$$\varepsilon_{x,0} = \frac{\partial u}{\partial x} \tag{3a}$$

$$\varepsilon_{\theta,0} = \frac{1}{R} \left( \frac{\partial v}{\partial \theta} + w \right) \tag{3b}$$

$$\gamma_{x\theta,0} = \frac{\partial v}{\partial x} + \frac{1}{R} \frac{\partial u}{\partial \theta} \tag{3c}$$

where R is radius of the shell. The changes in the curvature and torsion of the middle surface are [16]:

$$k_x = -\frac{\partial^2 w}{\partial x^2} \tag{4a}$$

$$k_\theta = -\frac{1}{R^2} \left( \frac{\partial^2 w}{\partial \theta^2} - \frac{\partial v}{\partial \theta} \right) \tag{4b}$$

$$k_{x\theta} = -\frac{2}{R} \left( \frac{\partial^2 w}{\partial x \partial \theta} - \frac{\partial v}{\partial x} \right) \tag{4c}$$

In this study, cross-ply and unidirectional lay-ups are considered; therefore

$$A_{16} = A_{26} = B_{16} = B_{26} = D_{16} = D_{26} = 0$$

The stiffnesses for composite laminated cylindrical shells can be written as:

$$A_{ij} = \sum_{k=1}^N Q_{ij}^k (h_k - h_{k-1}) \tag{5a}$$

$$B_{ij} = \frac{1}{2} \sum_{k=1}^N Q_{ij}^k (h_k^2 - h_{k-1}^2) \tag{5b}$$

$$D_{ij} = \frac{1}{3} \sum_{k=1}^N Q_{ij}^k (h_k^3 - h_{k-1}^3) \tag{5c}$$

where *h<sub>k</sub>* and *h<sub>k-1</sub>* are the distances of the middle surface of the shell to outer and inner surfaces of the *k<sub>th</sub>* layer, respectively.

In addition, *Q<sub>ij</sub><sup>k</sup>* denote the transformed reduced stiffness coefficients for the *k<sub>th</sub>* layer. Also, the stiffnesses for FML cylindrical shells are defined as following:

$$A_{ij} = Q_{ij}^m h_m + \sum_{k=1}^N Q_{ij}^k (h_k - h_{k-1}) \tag{6a}$$

$$B_{ij} = \frac{1}{2} \sum_{k=1}^N Q_{ij}^k (h_k^2 - h_{k-1}^2) \tag{6b}$$

$$D_{ij} = \frac{1}{12} Q_{ij}^m h_m^3 + \frac{1}{3} \sum_{k=1}^N Q_{ij}^k (h_k^3 - h_{k-1}^3) \tag{6c}$$

where *h<sub>m</sub>* and *Q<sub>ij</sub><sup>m</sup>* are the thickness and reduced stiffness of the metal layer. The governing equations of motion for thin cylindrical shell are obtained by introducing equation (2) into equation (1) as following:

$$\begin{aligned}
 & A_{11} \frac{\partial^2 u}{\partial x^2} + \frac{1}{R} A_{12} \left( \frac{\partial^2 v}{\partial x \partial \theta} + \frac{\partial w}{\partial x} \right) - B_{11} \frac{\partial^3 w}{\partial x^3} \\
 & + \frac{1}{R^2} B_{12} \left( -\frac{\partial^3 w}{\partial x \partial \theta^2} + \frac{\partial^2 v}{\partial x \partial \theta} \right) + \frac{1}{R} A_{66} \frac{\partial^2 v}{\partial x \partial \theta} \\
 & + \frac{1}{R^2} A_{66} \frac{\partial^2 u}{\partial \theta^2} + \frac{2}{R^2} B_{66} \left( -\frac{\partial^3 w}{\partial x \partial \theta^2} + \frac{\partial^2 v}{\partial x \partial \theta} \right)
 \end{aligned} \tag{7a}$$

$$\begin{aligned}
 & - \rho h \ddot{u} = 0 \\
 & A_{66} \frac{\partial^2 v}{\partial x^2} + \frac{1}{R} A_{66} \frac{\partial^2 u}{\partial x \partial \theta} + \frac{2}{R} B_{66} \left( -\frac{\partial^3 w}{\partial x^2 \partial \theta} + \frac{\partial^2 v}{\partial x^2} \right) \\
 & + \frac{1}{R} A_{12} \frac{\partial^2 u}{\partial x \partial \theta} + \frac{1}{R^2} A_{22} \left( \frac{\partial^2 v}{\partial \theta^2} + \frac{\partial w}{\partial \theta} \right) \\
 & - \frac{1}{R} B_{12} \frac{\partial^3 w}{\partial x^2 \partial \theta} + \frac{1}{R^3} B_{22} \left( -\frac{\partial^3 w}{\partial \theta^3} + \frac{\partial^2 v}{\partial \theta^2} \right)
 \end{aligned} \tag{7b}$$

$$\begin{aligned}
 & + \frac{1}{R} B_{66} \frac{\partial^2 v}{\partial x^2} + \frac{1}{R^2} B_{66} \frac{\partial^2 u}{\partial x \partial \theta} \\
 & + \frac{2}{R^2} D_{66} \left( -\frac{\partial^3 w}{\partial x^2 \partial \theta} + \frac{\partial^2 v}{\partial x^2} \right) + \frac{1}{R^2} B_{12} \frac{\partial^2 u}{\partial x \partial \theta} \\
 & + \frac{1}{R^3} B_{22} \left( \frac{\partial^2 v}{\partial \theta^2} + \frac{\partial w}{\partial \theta} \right) - \frac{1}{R^2} D_{12} \frac{\partial^3 w}{\partial x^2 \partial \theta} \\
 & - \frac{1}{R^4} D_{22} \frac{\partial^3 w}{\partial \theta^3} + \frac{1}{R^4} D_{22} \frac{\partial^2 v}{\partial \theta^2} - \rho h \ddot{v} = 0 \\
 & B_{11} \frac{\partial^3 u}{\partial x^3} + \frac{1}{R} B_{12} \left( \frac{\partial^3 v}{\partial x^2 \partial \theta} + \frac{\partial^2 w}{\partial x^2} \right) - D_{11} \frac{\partial^4 w}{\partial x^4} \\
 & + \frac{1}{R^2} D_{12} \left( -\frac{\partial^4 w}{\partial x^2 \partial \theta^2} + \frac{\partial^3 v}{\partial x^2 \partial \theta} \right) \\
 & + \frac{2}{R} B_{66} \frac{\partial^3 v}{\partial x^2 \partial \theta} + \frac{2}{R^2} B_{66} \frac{\partial^3 u}{\partial x \partial \theta^2} \\
 & + \frac{4}{R^2} D_{66} \left( -\frac{\partial^4 w}{\partial x^2 \partial \theta^2} + \frac{\partial^3 v}{\partial x^2 \partial \theta} \right) \\
 & + \frac{1}{R^2} B_{12} \frac{\partial^3 u}{\partial x \partial \theta^2} + \frac{1}{R^3} B_{22} \left( \frac{\partial^3 v}{\partial \theta^3} + \frac{\partial^2 w}{\partial \theta^2} \right) \\
 & - \frac{1}{R^2} D_{12} \frac{\partial^4 w}{\partial x^2 \partial \theta^2} + \frac{1}{R^4} D_{22} \left( -\frac{\partial^4 w}{\partial \theta^4} + \frac{\partial^3 v}{\partial \theta^3} \right) \\
 & - \frac{1}{R} A_{12} \frac{\partial u}{\partial x} - \frac{1}{R^2} A_{22} \left( \frac{\partial v}{\partial \theta} + w \right) + \frac{1}{R} B_{12} \frac{\partial^2 w}{\partial x^2} \\
 & + \frac{1}{R^3} B_{22} \left( \frac{\partial^2 w}{\partial \theta^2} - \frac{\partial v}{\partial \theta} \right) - \rho h \ddot{w} = 0
 \end{aligned} \tag{7c}$$

### 3. Analytical solution procedure

To obtain mode shapes, harmonic solution can be used. According to harmonic solution, in the first step space and time should be separated and then separation between axial and circumferential directions should be performed. Harmonic solution can be expressed as follows:

$$u(x, \theta, t) = U(x) \sin(n\theta) \sin(\omega t) \tag{8a}$$

$$v(x, \theta, t) = V(x) \cos(n\theta) \sin(\omega t) \tag{8b}$$

$$w(x, \theta, t) = W(x) \sin(n\theta) \sin(\omega t) \tag{8c}$$

where mode shapes in the longitudinal, torsional and flexural directions are denoted by  $U(x)$ ,  $V(x)$  and  $W(x)$ , respectively. In addition, the number of circumferential waves in the mode shape is shown by  $n$ . Also,  $\omega$  is the natural frequency of vibration. The three modal displacements are given by [16]:

$$\{U(x), V(x), W(x)\}^T = Ae^{\alpha z/R} \{C, B, 1\}^T \tag{9}$$

where  $\alpha$ ,  $A$ ,  $B$  and  $C$  are constants which are obtained as expressed in the follows. It should be mentioned that admittedly, the exact value of  $\alpha$  for cylindrical shells is unknown but it depends on the boundary conditions. The value of  $\alpha$  is related to the axial and circumferential modal numbers which can be specified by  $m$  and  $n$ , respectively. The value of  $\alpha$  is approximated by the beam so that the flexural mode shapes of the cylindrical shells in the axial direction are assumed in the identical form with the flexural vibration of beam subjected to the same boundary condition. Also, the values of  $A$ ,  $B$  and  $C$  which are modal displacements, are related to the modal frequency and system parameters. By introducing equations (8) and (9) into equation (7), a  $3 \times 3$  displacement coefficient matrix  $H$  in the non-dimensional form can be expressed as:

$$H_{3 \times 3} \{C, B, 1\}^T = \{0, 0, 0\}^T \tag{10}$$

where

$$\begin{aligned}
 H_{11} &= \alpha^2 - a_{66} n^2 + \Omega^2 \\
 H_{12} &= -H_{21} = -a_{12} n \alpha - b_{12} \frac{n \alpha}{R} \\
 &\quad - a_{66} n \alpha - 2b_{66} \frac{n \alpha}{R} \\
 H_{13} &= -H_{31} = a_{12} \alpha - b_{11} \frac{\alpha^3}{R} + b_{12} \frac{n^2 \alpha}{R} \\
 &\quad - 2b_{66} \frac{n^2 \alpha}{R} \\
 H_{22} &= a_{66} \alpha^2 + 2b_{66} \frac{\alpha^2}{R} - a_{22} n^2 - 2b_{22} \frac{n^2}{R} \\
 &\quad + b_{66} \frac{\alpha^2}{R} + 2d_{66} \left( \frac{\alpha}{R} \right)^2 - d_{22} \left( \frac{n}{R} \right)^2 + \Omega^2 \\
 H_{23} &= H_{32} = -2b_{66} \frac{\alpha^2 n}{R} + a_{22} n - b_{12} \frac{\alpha^2 n}{R} \\
 &\quad + b_{22} \frac{n^3}{R} - 2d_{66} \left( \frac{\alpha}{R} \right)^2 n + b_{22} \frac{n}{R} - d_{12} \left( \frac{\alpha}{R} \right)^2 n \\
 &\quad + d_{22} \frac{n^3}{R^2}
 \end{aligned} \tag{11}$$

$$H_{33} = 2b_{12} \frac{\alpha^2}{R} - d_{11} \frac{\alpha^4}{R^2} + 2d_{12} \left( \frac{n\alpha}{R} \right)^2 + d_{66} \left( \frac{2n\alpha}{R} \right)^2 - 2b_{22} \frac{n^2}{R} - d_{22} \frac{n^4}{R^2} - a_{22} + \Omega^2$$

where

$$\begin{aligned} a_{12} &= \frac{A_{12}}{A_{11}} & a_{22} &= \frac{A_{22}}{A_{11}} & a_{66} &= \frac{A_{66}}{A_{11}} \\ b_{11} &= \frac{B_{11}}{A_{11}} & b_{12} &= \frac{B_{12}}{A_{11}} & b_{22} &= \frac{B_{22}}{A_{11}} \\ b_{66} &= \frac{B_{66}}{A_{11}} & d_{11} &= \frac{D_{11}}{A_{11}} & d_{12} &= \frac{D_{12}}{A_{11}} \\ d_{22} &= \frac{D_{22}}{A_{11}} & d_{66} &= \frac{D_{66}}{A_{11}} \end{aligned} \quad (12)$$

The determinant of coefficient matrix H set to zero to for each value of n for a non-trivial solution of the equations of motion. When the value of  $\alpha$  is provided, the displacement coefficient matrix leads to a six-order polynomial in  $\omega$ .

#### 4. Results of free vibration

In this section, there is comparison between free vibration of FML and composite circular cylindrical shells subjected to different boundary conditions. The obtained results of beam modal function for composite circular cylindrical shells with  $L/R=1, 5$  and  $10$  are compared with the exact results [18] for verifying the accuracy of the proposed analytical solution.

##### 4.1. Validation

To validate the beam modal function method, the obtained non-dimensional frequency parameter  $\Omega = \omega \sqrt{\rho R^2 / E_{22}}$  is compared with the exact solution. The shown comparison in Table 1 is carried out for cross/ply  $[0^\circ / 90^\circ / 0^\circ]$  composite laminated cylindrical shells with material properties  $E_2 = 7.6(GPa)$ ,  $G_{12} = 4.1(GPa)$ ,  $E_1/E_2 = 2.5$  and  $\nu_{12} = 0.26$  with different n and  $L/R=10$  subjected to simply supported boundary condition. The comparison indicates that the presented method has excellent agreement with the exact solution.

##### 4.2. Comparison between free vibration analysis of FML and composite cylindrical shells

The effects of different parameters such as material properties, boundary condition, axial and circumferential modal numbers and lay-ups on the frequencies of the FML and composite cylindrical shells is studied and compared in this section. The lay-ups of FML and composite cylindrical shells are considered four  $[Al/0^\circ / 90^\circ / 0^\circ]$  and three-layered  $[0^\circ / 90^\circ / 0^\circ]$ , respectively, and  $L/R=10, h/R=0.002$  as shown in Figure 1. Further, the considered material properties of aluminium, carbon/epoxy and glass/epoxy are shown in Table 2.

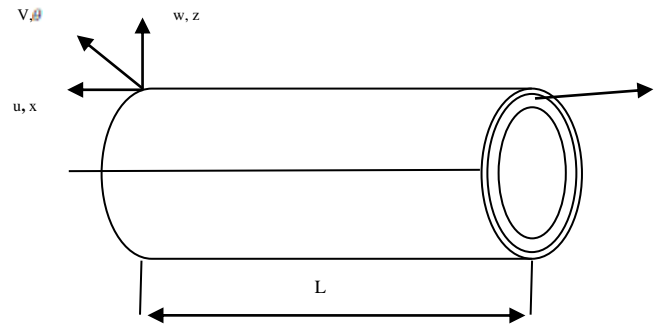


Figure 1a. FML cylindrical shell

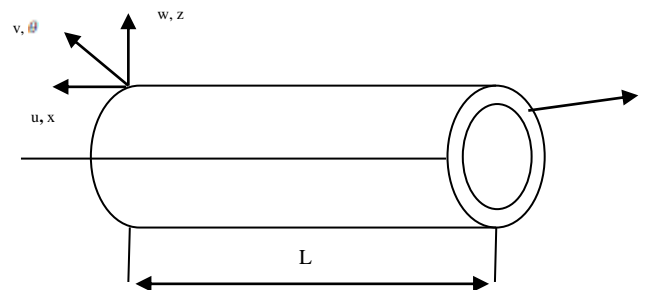


Figure 1b. Composite cylindrical shell

**Table 1.** Comparison of the non-dimensional frequencies for a composite cylindrical shell with simply supported boundary condition ( $m=1$ )

$n$	Present	Exact solution [18]
1	0.083908	0.083908
2	0.030009	0.030009
3	0.015193	0.015193
4	0.012176	0.012176
5	0.015231	0.015231
6	0.021179	0.021179

**Table 2.** Material properties of aluminium, carbon/epoxy and glass/epoxy

Materials	properties				
	$E_x(GPa)$	$E_y(GPa)$	$E_s(GPa)$	$\nu_x$	$\rho(Kg/m^3)$
Aluminum alloy 2024-T3	72.4	72.4	28	0.33	2700
Carbon/epoxy	181	10.3	7.17	0.28	1600
Glass/epoxy	38.6	8.27	4.14	0.26	1800

As depicted in Figure 2, the non-dimensional frequencies of FML and composite cylindrical shells subjected to different  $n$  and material properties with simply supported boundary condition are obtained. It can be seen that the frequencies of carbon/epoxy are greater than glass/epoxy for all of the  $n$ , because carbon/epoxy is more stiff than glass/epoxy. This process is not constant for FML because of metal existence. Although the frequencies of CARALL are more than GLARE for  $n < 5$ , this process is converted. It means that the frequencies of GLARE are greater than CARALL for  $n > 5$ .

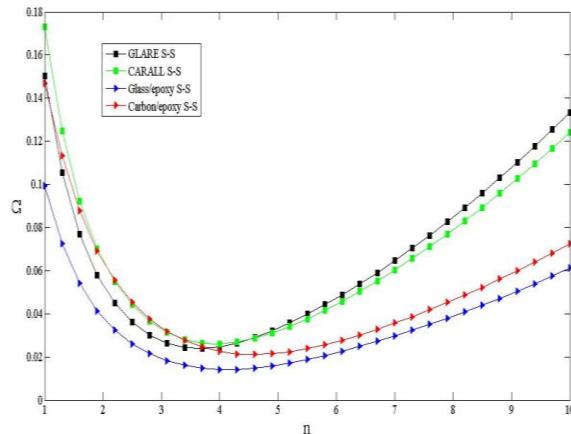


**Figure 2.** Comparison between non-dimensional frequencies of FML and composite cylindrical shells with respect to  $n$  for different material properties

The non-dimensional frequencies of FML and composite cylindrical shells with respect to  $n$  for different  $m$  are compared in Figure 3. As shown in the figure, both FML and composite cylindrical shells are converged with growing  $n$ . Although both structures are converged with growing  $n$ , CARALL is converged faster than carbon/epoxy. Moreover, the frequencies of CARALL are often greater than carbon/epoxy because with adding the metal layer to the composite cylindrical shell, the stiffness of cylindrical shell increases. Also, the frequencies of both structures for  $m=2$  are more than  $m=1$ .

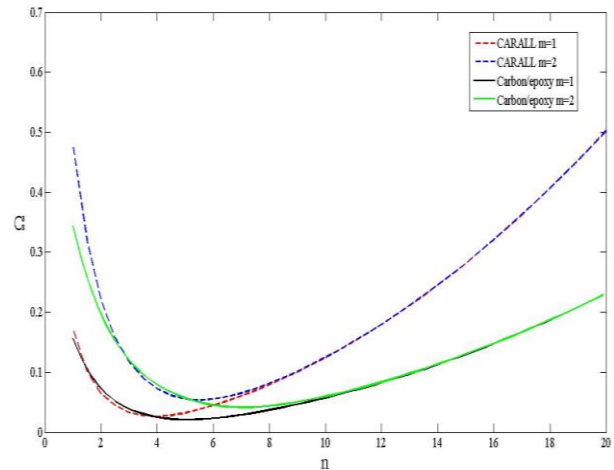


**Figure 3.** Comparison between non-dimensional frequencies of FML and composite cylindrical shells with respect to  $n$  for different  $m$

The non-dimensional frequencies of FML and composite cylindrical shells for different lay-ups are indicated in Figure 4. It can be seen that the frequencies of CARALL are greater than carbon/epoxy for both lay-ups. In addition, the frequencies of unidirectional are more than the cross-ply for both FML and composite in the less  $n$  because of more stiffness of unidirectional lay-up, but with increasing the  $n$ , this procedure is converted. Further, the frequencies of CARALL for both lay-ups are near to each other, but the frequencies of carbon/epoxy for unidirectional and cross-ply lay-ups become away from each other with raising the  $n$ .

A comparison between the boundary conditions of CARALL and carbon/epoxy are considered in the Figure 5. As predicted, the frequencies of clamped boundary condition are more than the simply supported boundary condition for both FML and composite structures since the clamped boundary condition fix the boundaries of the cylinder in all of the directions. Furthermore, the frequencies of FML are greater than the composite one for all of the  $n$  because the FML is stiffer than the composites due to the existence of metal layer. Also, the frequencies of both boundary conditions are converged with increasing  $n$  for both FML and composite cylindrical shells. The

effect of length to radius ratio on the frequencies of FML and composite cylindrical shells for different  $m$  are demonstrated in Figure 6. As shown in the figure, with growing the  $L/R$ , the frequencies of both structures are decreased. With increasing the  $L/R$ , the frequencies of CARALL and carbon/epoxy are converged for both  $m=1$  and  $m=2$ .

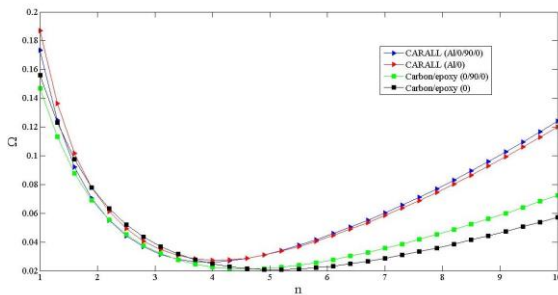


**Figure 4.** Comparison between non-dimensional frequencies of FML and composite cylindrical shells with respect to  $n$  for different lay-ups

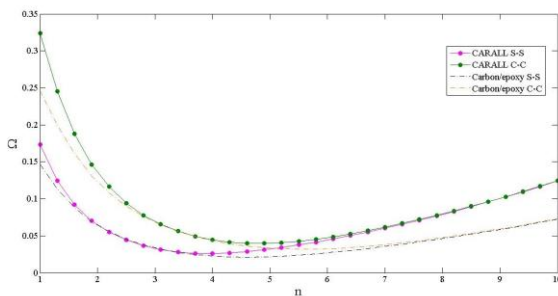


**Figure 5.** Comparison between non-dimensional frequencies of FML and composite cylindrical shells with respect to  $n$  for different boundary conditions

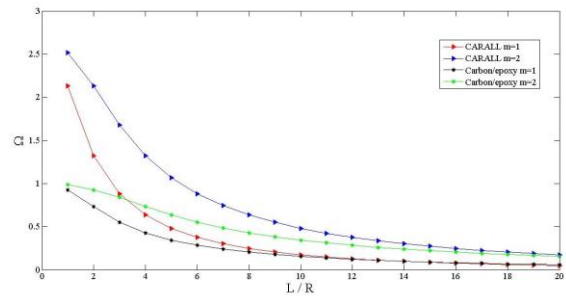


**Figure 6.** Comparison between non-dimensional frequencies of FML and composite cylindrical shells with respect to  $L/R$  for different  $m$

### 5. Conclusion

In this manuscript, free vibrations of FML and composite cylindrical shells subjected to different boundary conditions using beam modal function method have been compared to each other. Love's first approximation theory has been applied to obtain the equations of motion for these cylindrical shells. Carbon/epoxy and glass/epoxy have been studied for the composite section and aluminium has been considered for the metal section. The results demonstrated constant process for composite cylinder and inconstant process for FML one. The frequencies of carbon/epoxy are more than glass/epoxy for all of the  $n$ , but the frequencies of CARALL are more and less than GLARE for  $n < 5$  and  $n > 5$ , respectively. Also, admittedly both FML and composite structures are converged with growing  $n$ , but CARALL is converged faster than carbon/epoxy. Moreover, the frequencies of both boundary conditions are converged with increasing  $n$  for both FML and composite cylindrical shells.

### References

1. Ghasemi A.R., Taheri-Behrooz F., Farahani S.M.N., Mohandes M., 2016, Nonlinear free vibration of an Euler-Bernoulli composite beam undergoing finite strain subjected different boundary conditions, *Journal of Vibration and Control* 22(3): 799-811.
2. Mohandes M., Ghasemi A.R., 2016, Finite strain analysis of nonlinear vibrations of symmetric laminated composite Timoshenko beams using generalized differential quadrature method, *Journal of Vibration and Control* 22(4): 940-954.
3. Ghasemi A.R., Mohandes M., 2017, Nonlinear free vibration of laminated composite Euler-Bernoulli beams based on finite strain using GDQM, *Mechanics of Advanced Materials and Structures* 24(11): 917-923.
4. Ghasemi A.R., Mohandes M., 2017, Modified couple stress theory and finite strain assumption for nonlinear free vibration and bending of micro/nanolaminated composite Euler-Bernoulli beam under thermal

- loading, Part C: *Journal of Mechanical Engineering Science* 231(21): 4044-4056.
5. Goodarzi M., Nikkhal Bahrami M., Tavaf V., 2017, Refined plate theory for free vibration analysis of FG nanoplates using the nonlocal continuum plate model, *Journal of Computational Applied Mechanics* 48(1): 123-136.
6. Shishesaz M., Kharazi M., Hosseini P., Hosseini M., 2017, Buckling Behavior of Composite Plates with a Pre-central Circular Delamination Defect under in-Plane Uniaxial Compression, *Journal of Computational Applied Mechanics* 48(1): 111-122.
7. Fazzolari F.A., 2014, A refined dynamic stiffness element for free vibration analysis of cross-ply laminated composite cylindrical and spherical shallow shells, *Composites Part B: Engineering* 62: 143-158.
8. Sofiye A.H., Kuruoglu N., 2014, Buckling and vibration of shear deformable functionally graded orthotropic cylindrical shells under external pressures, *Thin-Walled Structures* 78: 121-130.
9. Ghorbanpour Arani A., Haghparast E., Khoddami Maraghi Z., 2015, Vibration analysis of double bonded

- composite pipe reinforced by BNNTs conveying oil, *Journal of Computational Applied Mechanics* 46: 93-105.
10. Xie X., Jin G., Yan Y., Shi S.X., Liu Z., 2014, Free vibration analysis of composite laminated cylindrical shells using the Haar wavelet method, *Composite Structures* 109: 169-177.
  11. Song Z.G., Zhang L.W., Liew K.M., 2016, Vibration analysis of CNT-reinforced functionally graded composite cylindrical shells in thermal environments, *International Journal of Mechanical Sciences* 115-116: 339-347.
  12. Ansari R., Torabi J., 2016, Numerical study on the buckling and vibration of functionally graded carbon nanotube-reinforced composite conical shells under axial loading, *Composites Part B: Engineering* 95: 196-208.
  13. Xiang X., Guoyong J., Wanyou L., Zhigang L., 2014, A numerical solution for vibration analysis of composite laminated conical, cylindrical shell and annular plate structures, *Composite Structures* 111: 20-30.
  14. Tornabene F., Fantuzzi N., Baccocchi M., Dimitri R., 2015, Free vibrations of composite oval and elliptic cylinders by the generalized differential quadrature method, *Thin-Walled Structures*, 97: 114-129.
  15. Bidgoli A.M.M., Heidari-Raran M., 2016, Axial buckling response of fiber metal laminate circular cylindrical shells, *Structural Engineering and Mechanics* 57(1): 45-63.
  16. Mohandes M., Ghasemi A.R., Irani-Rahagi M., Torabi K., Taheri-Behrooz F., 2017, Development of beam modal function for free vibration analysis of FML circular cylindrical shells, *Journal of Vibration and Control* doi: 10.1177/1077546317698619.
  17. Ghasemi A.R., Mohandes M., 2017, Free vibration analysis of rotating fiber-metal laminate circular cylindrical shells, *Journal of Sandwich Structures and Materials* doi: 10.1177/1099636217706912.
  18. Lam K.Y., Loy C.T., 1995, Analysis of rotating laminated cylindrical shells by different shell theories, *Journal of Sound and Vibration* 186(1): 23-35.